Max-Planck-Institut
für Mathematik
in den Naturwissenschaften
Leipzig

Self-similar folding patterns and energy scaling in compressed elastic sheets

by

Sergio Conti, Antonio DeSimone, and Stefan Müller

Preprint no.: 3 2004

Self-similar folding patterns and energy scaling in compressed elastic sheets

Sergio Conti,[1] Antonio DeSimone[2] and Stefan Müller[1]

[1] *Max-Planck-Institute for Mathematics in the Sciences, Inselstr. 22-26, 04103 Leipzig, Germany*
[2] *SISSA-International School for Advanced Studies, Via Beirut 2-4, 34014 Trieste, Italy*

January 12, 2004

Thin elastic sheets under isotropic compression, such as for example blisters formed by thin films which debonded from the substrate, can exhibit remarkably complex folding patterns. We discuss the scaling of the elastic energy with respect to the film thickness, and show that in certain regimes the optimal energy scaling can be reached by self-similar folding patterns that refine towards the boundary, in agreement with experimental observations. We then extend the analysis to anisotropic compression, and discuss a simplified scalar model which suggests the presence of a transition between a regime where the deformation is governed by global properties of the domain and another one where the direction of maximal compression dominates and the scale of the folds is mainly determined by the distance to the boundary in the direction of the folds themselves.

1 Introduction

Debonding from the substrate and subsequent blistering is a mechanism by which a film can release compressive stresses. This happens for example upon cooling films deposited at high temperature on a substrate with a larger thermal expansion coefficient, see [31] for a review of the experimental context and of the technological applications. The complexity of the resulting patterns have generated interest spanning the mechanics [10, 48, 31, 4], physics [46, 39, 7, 54, 53, 3, 12] and mathematics [2, 33, 8, 24, 34, 35, 9] literature. Experimentally, typical observed configurations exhibit folds perpendicular to the boundary, which often coarsen in the interior of the debonded region, see for example [1, 31]. In many cases even the debonded region itself has a complex shape, as for example in the so-called *telephone-cord blisters* [48, 31]. Theoretically, the analysis of such phenomena is typically based on a separa-

tion of time scales. A fast elastic relaxation determines the folding pattern of the debonded region. The debonded region itself arises and grows by means of a slower fracture process whose driving force is given by the solution of the elasticity problem. We focus here on the first, elastic, problem, and assume the debonded region to be fixed. Our results show that oscillations spontaneously form close to the boundary, even if the boundary itself is straight. This implies that the driving force for boundary propagation is oscillatory, and therefore that straight boundaries will tend, after propagation, to become wavy. This argument indicates that the waviness of the boundary is a consequence of the formation of oscillations in the elastic problem in the interior, and not vice versa, as often assumed in the literature on the subject. This effect, which had already been mentioned in [48], was studied within a linear stability analysis by Audoly in [3].

We briefly review in Section 2 several simplified two-dimensional models for elasticity of thin sheets and their derivations from three-dimensional elasticity. Then, in Section 3 we discuss the patterns expected for isotropically compressed films. The heuristic discussion is based on a two-dimensional vectorial model, but all results hold for the full three-dimensional elasticity theory. Section 4 is focussed on the case of anisotropic compression, within a restricted scalar model.

2 Reduced two-dimensional models

Let $\omega \subset \mathbb{R}^2$ be the region where the film detached from the substrate, which we assume to be smooth and bounded, and $h > 0$ be the film thickness. Then, the deformation $\phi : \omega \times (0,h) \to \mathbb{R}^3$ is determined by minimization of the elastic energy

$$I^h_{3\mathrm{D}}[\phi] = \frac{1}{h} \int_{\omega\times(0,h)} W_{3\mathrm{D}}(\nabla\phi)\, dx\,, \tag{1}$$

where the free-energy density $W_{3\mathrm{D}}(F)$ behaves qualitatively as the squared distance of F from the set $SO(3)$ of rotations (our more general precise assumptions are stated below). The boundary conditions are set by the part of the film which is still bound to the substrate, and are given by

$$\phi(x) = \begin{pmatrix} (1-\epsilon_*)x_1 \\ (1-\epsilon_*)x_2 \\ x_3 \end{pmatrix} \text{ on } (\partial\omega)\times(0,h) \tag{2}$$

where $\epsilon_* > 0$ is a small parameter representing the amount of compression. As usual in thin-film elasticity boundary conditions are imposed only on the lateral boundary, not on the top and bottom faces of the sheet.

2.1 A director ansatz

The history of the theory of thin sheets and shells is paved with a number of simplifications of the general elasticity functional (1) aiming at a direct description of the behavior of the sheet as a two-dimensional object, without resolving explicitly the third dimension. The model of choice for the blistering problem is the von Kármán functional, where both stretching and bending of the film are included. This can be heuristically derived by means of an *ansatz*, due to Kirchhoff, which enslaves the three-dimensional deformation ϕ to the behavior of the mid-plane section ψ. Namely, given $\psi : \omega \to \mathbb{R}^3$, one writes

$$\phi(x_1, x_2, x_3) = \psi(x_1, x_2) + x_3 b(x_1, x_2)$$

and then optimizes locally over all vectors fields $b \in \mathbb{R}^3$. Within a formal asymptotic expansion, and up to multiplicative coefficients, the optimal choice for b is the normal ν to the surface described by ψ, defined according to

$$\nu = \frac{\psi_{,1} \wedge \psi_{,2}}{|\psi_{,1} \wedge \psi_{,2}|} \,.$$

In materials with a nonzero Poisson's ratio the energy can be further reduced by including the second-order term in x_3. Since it does not change the energy scaling, for simplicity we neglect this correction. A formal asymptotic expansion leads then to the reduced energy (again, up to inessential multiplicative factors of order unity)

$$I^h_{2\mathrm{D}}[\psi] = \int_\omega W_{2\mathrm{D}}(\nabla\psi) + h^2 |\nabla\nu|^2 \, dx \tag{3}$$

where $|\nabla\nu|^2 = |\partial_1\nu|^2 + |\partial_2\nu|^2$. The new potential $W_{2\mathrm{D}}(a|b)$ is obtained from $W_{3\mathrm{D}}(a|b|c)$ by optimizing over all possible choices for the third column c of the argument,

$$W_{2\mathrm{D}}(F) = \min_{c\in\mathbb{R}^3} W_{3\mathrm{D}}(F|c) \,, \qquad F \in \mathbb{R}^{3\times 2} \,.$$

Here $(F|c)$ denotes the 3×3 matrix obtained extending F with c in the third column, $Fe_1 \otimes e_1 + Fe_2 \otimes e_2 + c \otimes e_3$. This definition is, for low-energy and smooth deformations, equivalent to the one obtained by simply assuming that c is a unit vector normal to the first two columns of F, i.e. $c = \nu$. The function $W_{2\mathrm{D}}(F)$ is therefore equivalent to the squared distance of F from the set $O(2,3)$ of linear isometries from $\mathbb{R}^2$ to $\mathbb{R}^3$.

2.2 Rigorous results on membrane and plate theories

The method of choice for the mathematical derivation of reduced variational theories is Gamma convergence, a criterion for convergence of functionals which is naturally coupled to convergence of minimizers, developed by De Giorgi and his school in the 70s ([22]; see also [21, 11]). Recent progress in the mathematical theory of thin elastic bodies has shown that each of the two terms that form the model (3) can be, separately and in different regimes, justified by means of Gamma convergence. No such result exists, however, for $I_{2\mathrm{D}}$, and indeed this approach by Gamma convergence seems unable to derive a functional such as (3) where the small parameter does not disappear in the limit, but is still present in front of a term with higher derivatives (mathematically, a problem with a singular perturbation).

The first term in (3), called the stretching term, is characteristic of membrane theories, which are written in terms of the first gradient of the deformation. Convergence of the three-dimensional problem to a membrane theory was proven by LeDret and Raoult [42, 43, 44], who (under some technical growth conditions on $W_{3\mathrm{D}}$) showed that the Gamma-limit of $I^h_{3\mathrm{D}}[\phi]$, as $h \to 0$, is given by

$$I_{\mathrm{membrane}}[\psi] = \int_\omega W^{\mathrm{qc}}_{2\mathrm{D}}(\nabla\psi)\, dx$$

where $\psi : \omega \to \mathbb{R}^3$ is the limit of the vertical averages of ϕ, in the sense that

$$\frac{1}{h}\int_0^h \phi(x_1, x_2, x_3)dx_3 \to \psi(x_1, x_2)$$

in L^2. The reduced energy density $W^{\mathrm{qc}}_{2\mathrm{D}} : \mathbb{R}^{3\times 2} \to \mathbb{R}$ is the quasiconvex envelope of the reduction $W_{2\mathrm{D}}$ of the elastic energy density $W_{3\mathrm{D}}$ to two dimensions. Precisely, it corresponds to optimizing $W_{2\mathrm{D}}$ over all possible oscillations which can be realized by gradient fields with affine boundary data, according to

$$W^{\mathrm{qc}}_{2\mathrm{D}}(F) = \inf\left\{\int_{(0,1)^2} W_{2\mathrm{D}}(F + \nabla v)dx : \quad v \in C^\infty_0((0,1)^2)\right\}.$$

A simple computation shows that since the function $W_{3\mathrm{D}}$ vanishes on $SO(3)$, the two-dimensional energy $W_{2\mathrm{D}}$ vanishes on $O(2,3)$, and the envelope $W^{\mathrm{qc}}_{2\mathrm{D}}$ vanishes on convex hull of $O(2,3)$, which is given by the set of all *short* matrices, i.e. of all matrices $F \in \mathbb{R}^{3\times 2}$ such that $F^TF \leq \mathrm{Id}$ (equivalently, the nonlinear strain is compressive, i.e. both singular values of F are less than or equal to 1). This behavior is remarkably different from what happens in the first term of the reduced theory defined in (3): the latter only vanishes

on gradients of isometric maps, not on all compressive strains. This difference arises from the fact that in the scaling regime considered by LeDret and Raoult fine-scale oscillations which can absorb compressive strains can be generated at no energetic cost, since no bending term is present. Mechanically, this reflects the fact that the sheet cannot withstand compression. The resulting tension-field theory had been discussed earlier by Pipkin [52, 51].

The second term in (3), called the bending term, is characteristic of plate theories, and it was considered by Friesecke, James and Müller [28, 29] and by Pantz [49, 50]. They have shown that the Gamma-limit of $h^{-2} I^h_{\rm 2D}[\phi]$, as $h \to 0$, is given by a functional which had been proposed with a heuristic derivation by Kirchhoff in 1850 [36], namely,

$$I_{\rm plate}[\psi] = \begin{cases} \displaystyle\int_\omega Q_2(II\psi)\,dx & \text{if } \psi \in W^{2,2}(\omega,\mathbb{R}^3),\ \ \nabla\psi \in O(2,3) \\ \infty & \text{else.} \end{cases}$$

Here $II\psi$ denotes the second fundamental form of ψ, which can be defined as the projection on the tangent space to the surface described by ψ of the gradient of the normal to such surface, i.e.,

$$II\psi = (\nabla\psi)^T \nabla\nu\,, \qquad \nu = \frac{\psi_{,1}\wedge\psi_{,2}}{|\psi_{,1}\wedge\psi_{,2}|}\,.$$

The quadratic form $Q_2(G)$ is defined on $\mathbb{R}^{2\times 2}$ by

$$Q_2(G) = \frac{1}{24}\min_{b\in\mathbb{R}^3} Q_3(G|b)\,, \qquad Q_3(F) = \frac{\partial^2 W_{\rm 3D}}{\partial F^2}({\rm Id})(F,F)\,.$$

The components of the quadratic form Q_3 are the elastic constants of the material, and the optimization in b is analogous to the one that leads from $W_{\rm 3D}$ to $W_{\rm 2D}$ in the membrane theory. The resulting model $I_{\rm plate}$ is very rigid. In fact, the energy is infinite for all deformations which are not $W^{2,2}$-smooth local isometries, which leaves rather little freedom.

Both mentioned results, namely, the rigorous derivation of membrane and plate theories, have represented substantial progress in the mathematical understanding of thin elastic bodies. However, none of them permits to make any prediction for the blistering problem of interest here. Precisely, the functional $I_{\rm membrane}$ vanishes on all maps which are short, such as for example the affine continuation of the boundary data. The functional $I_{\rm plate}$ instead is infinite on all maps that satisfy the boundary conditions. None of the two gives useful information on the blistering patterns. In particular, the functional $I_{\rm 2D}$ defined in (3) is *not* equivalent to $\tilde I = I_{\rm membrane} + h^2 I_{\rm plate}$: the latter is indeed finite only on locally isometric maps, whereas $I_{\rm 2D}$ is

finite on all twice differentiable fields ψ. In particular, for the affine map $\psi_a(x) = ((1-\epsilon_*)x, 0)$, which satisfies the boundary conditions of the blistering problem, we obtain that $I_{2D}(\psi_a)$ behaves as $c|\omega|{\epsilon_*}^2$, whereas $\tilde{I}(\psi_a) = \infty$.

The reduced model (3) still contains the small parameter h. In mathematical terms, the bending correction, which corresponds to a term depending on the second derivative of ψ, represents a singular perturbation. From the point of view of elasticity, the peculiarity of the blistering problem is that both the stretching term – depending on $\nabla\psi$ – and the bending term – depending on $\nabla\nu$ – are present and relevant, but they appear with very different coefficients. We remark that the geometrically linearized version of the model (3), corresponding to the von Kármán model, has been derived first formally by asymptotic expansion [16, 17] and then rigorously by Gamma convergence [27] and alternatively by a subtle application of the implicit function theorem [47] in a scaling regime where both terms have the same behavior, hence in which no small parameter appears in the limit. This corresponds to energies scaling as the fifth power of the film thickness, and is not relevant for the blistering problem.

2.3 The scalar ansatz

The functional I_{2D} can be further simplified by assuming that the deformations are small, which leads to a geometrically linear model which we do not discuss here. Ortiz and Gioia proposed in 1994 [48] a more drastic simplification, namely, they assumed that only the component of ψ normal to the plane is active, in the sense that

$$\psi(x) = \begin{pmatrix} (1-\epsilon_*)x \\ w(x) \end{pmatrix}$$

where $w : \omega \to \mathbb{R}$ is a scalar deformation field. This leads to a simplified scalar model, which after suitable rescaling (see below) takes the form

$$I_{\mathrm{Eik}}[u] = \int_\omega \left[(\nabla u)^2 - 1\right]^2 + \sigma^2 |\nabla^2 u|^2 \, dx \,, \tag{4}$$

where $\sigma = h/(2\epsilon_*)^{1/2}$ is the natural length scale of the problem.The functional I_{Eik} also plays a role in models of liquid crystals [5], of micromagnetism in thin films [24, 25], and of convection patterns in fluids [26]. In spite of recent progress (see [2, 6, 33, 24, 23]) the Gamma limit of I_{Eik} as $\sigma \to 0$ remains to be identified. The natural candidate low-energy state of I_{Eik} is obtained setting $u(x)$ equal to the distance of x from the boundary of ω, and then smoothing it where the gradient jumps. This approximate solution, that

was first proposed by Gioia and Ortiz, leads to a scaling of the total elastic energy per unit thickness of the form $c|\omega| + ch{\epsilon_*}^{3/2}$. We shall show later that this energy is not optimal, in the sense that inclusion of the in-plane components permits to relax the energy down to order $ch{\epsilon_*}^{3/2}$, eliminating the constant term. Further, the mentioned scalar approach and its solution $w(x) \simeq \mathrm{dist}(x, \partial\omega)$ indicate that the folding patterns in the interior of the domain arise as a consequence of the waviness of the boundary. In particular, in a domain with smooth boundaries very few folds on a long length scale are expected; for example, only a segment in an ellipse, or the two diagonals in a square (see Figure 1). We shall argue later that inclusion of the tangential components permits to identify the formation of a large number of additional folds on a much finer length scale, which refine towards the boundary. For the case of anisotropically compressed films, however, our discussion is restricted to the simplified scalar model.

3 Folding patterns in compressed thin films

We study the qualitative properties of low-energy states of the three-dimensional elasticity problem (1) under compressive affine boundary conditions as specified in (2). The heuristic discussion will be phrased in terms of the more explicit two-dimensional reduced functional (3). We remark that all results presented here apply to the full problem (1) (see [9]), the reduction to two dimensions is only used for the purpose of a more explicit heuristic derivation and a simpler pictorial illustration. As mentioned above, the three-dimensional energy density $W_{3\mathrm{D}}$ is locally comparable to the squared distance from the set $SO(3)$ of rotations, and the two-dimensional energy density $W_{2\mathrm{D}}$ is locally comparable to the squared distance from the set $O(2,3)$ of linear isometric maps from $\mathbb{R}^2$ to $\mathbb{R}^3$. For simplicity of notation we shall formulate our statements under the assumption that the reduced two-dimensional energy takes the specific form

$$W_{2\mathrm{D}}(F) = \mathrm{dist}^2(F, O(2,3))\,.$$

The entire argument applies, however, to general energy densities which satisfy the growth conditions stated in (8-9) below.

A first approximation to the solution, which corresponds to the scalar model discussed in the introduction, can be obtained by relaxing only the vertical component, i.e. optimizing over all deformations of the form

$$\psi_{\mathrm{scal}}(x) = \begin{pmatrix} (1-\epsilon_*)x \\ w(x) \end{pmatrix}\,. \tag{5}$$

Here and below we use x to denote two-dimensional coordinates, $x = (x_1, x_2) \in \omega \subset \mathbb{R}^2$. Computing the gradient of $\psi_{\rm scal}$ we get

$$\nabla\psi_{\rm scal}^T \nabla\psi_{\rm scal} = (1-\epsilon_*)^2 {\rm Id} + \nabla w \otimes \nabla w \,.$$

Matrices F in $O(2,3)$ are characterized by the fact that $F^T F = {\rm Id}$, and, indeed, $W_{\rm 2D}(F)$ behaves as $|F^T F - {\rm Id}|^2$ for matrices F close to the identity. Therefore the energy density $W_{\rm 2D}(\nabla\psi_{\rm scal})$ is comparable to

$$|\nabla\psi_{\rm scal}^T \nabla\psi_{\rm scal} - {\rm Id}|^2 = |\nabla w \otimes \nabla w - (2\epsilon_* + {\epsilon_*}^2){\rm Id}|^2 \,.$$

No multiple of the rank-one matrix $\nabla w \otimes \nabla w$ can equal the rank-two matrix $(2\epsilon_* + {\epsilon_*}^2){\rm Id}$, hence no choice of w permits to relax locally the energy to zero. However, writing $w(x) = (2\epsilon_* + {\epsilon_*}^2)^{1/2} u(x)$ the expression above takes the simplified form

$$|\nabla\psi_{\rm scal}^T \nabla\psi_{\rm scal} - {\rm Id}|^2 = (2\epsilon_* + {\epsilon_*}^2)^2 \left[1 + (|\nabla u|^2 - 1)^2\right] \,,$$

hence compression in one direction is relaxed if $|\nabla u| = 1$. This condition corresponds to the eikonal equation, and a solution to it which satisfies the required boundary condition $u = 0$ on $\partial\omega$ is obtained by setting $u(x) = {\rm dist}(x, \partial\omega)$. This shows that optimization within this restricted class permits to relax an isotropic compression to a uniaxial one, thereby reducing the stored energy by a factor two, in the sense that a deformation of the form (5) with $|\nabla u| = 1$ has half the energy of the one with $u = 0$. The resulting deformation is illustrated for the case of a square in Figure 1. Here the gradient of u is a unit vector parallel to e_1 or e_2, constant in four parts of the domain. The corresponding symmetrized strain takes the form

$$\nabla\psi_{\rm scal}^T \nabla\psi_{\rm scal} = \begin{pmatrix} 1-(2\epsilon_* + {\epsilon_*}^2) & 0 \\ 0 & 1 \end{pmatrix} \quad \text{or} \quad \begin{pmatrix} 0 & 1 \\ 1-(2\epsilon_* + {\epsilon_*}^2) & 0 \end{pmatrix}$$

in the different parts of the domain, corresponding to a uniaxial compression. Note that the remaining compression is uniaxial everywhere, but it is not everywhere in the same direction, therefore it has to be treated separately in the different parts of the domain. The procedure just described corresponds to the Gioia-Ortiz approximation [48]. In the next sections we refine this construction, showing how the remaining uniaxial compression in the orthogonal direction can be relaxed.

3.1 Energy relaxation by one-dimensional folds and a boundary layer

Uniaxial compression in a flat domain can be relaxed by means of a cylindrical deformation containing smooth fine-scale oscillations, as illustrated

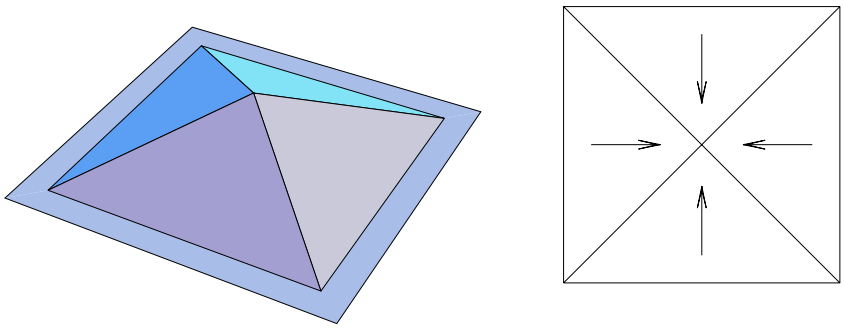

(a) (b)

FIGURE 1: (a): Piecewise affine deformation relaxing an isotropic biaxial compression to a uniaxial one in the unit square. (b): the gradient of w in the three pieces. In each triangle, compression parallel to the corresponding part of the boundary is unrelaxed.

in Figure 2. If the oscillation scale is fine enough, it is possible to insert a small-energy boundary layer to achieve Dirichlet boundary conditions and/or to patch together oscillations with different orientations. To give a precise construction of the oscillatory map we choose a smooth curve $\gamma : \mathbb{R} \to \mathbb{R}^2$ which is parameterized by arc length (i.e. $|\gamma'| = 1$ everywhere) and satisfies

$$\gamma(t+1) = \gamma(t) + \begin{pmatrix} 1-\epsilon_* \\ 0 \end{pmatrix}$$

(see e.g. Figure 2a). It is easy to see that the function γ can be chosen so that the distance from a straight line is controlled by

$$|\gamma_1(t) - (1-\epsilon_*)t| \leq c\epsilon_* \,, \qquad |\gamma_2(t)| \leq c{\epsilon_*}^{1/2}$$

and analogous bounds on the first and second derivatives, much as in the analysis of Euler buckling of compressed rods. Given a period $p > 0$ to be chosen later, we set

$$\psi_p(x) = \begin{pmatrix} x_1 \\ p\gamma_1(x_2/p) \\ p\gamma_2(x_2/p) \end{pmatrix}$$

where we assumed for definiteness that the uniaxial compression is in the x_2 direction. The resulting deformation is illustrated in Figure 2b. The map ψ_p achieves *on average* the uniaxial compression

$$F = \begin{pmatrix} 1 & 0 \\ 0 & 1-\epsilon_* \\ 0 & 0 \end{pmatrix} \,,$$

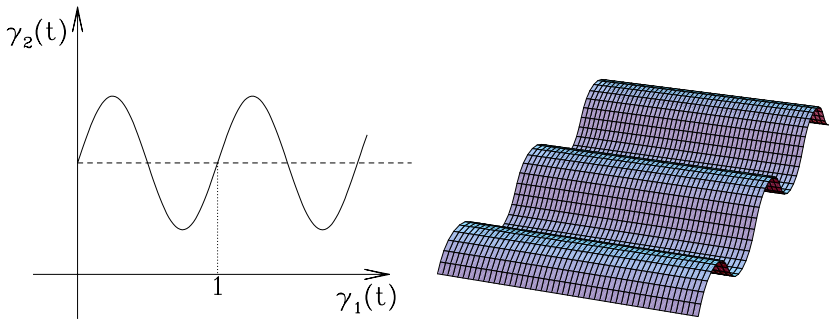

(a) (b)

FIGURE 2: One-dimensional periodic profile, corresponding to uniaxial compression, as in Euler buckling. (a): the curve $\gamma(t)$. (b): the corresponding deformation ψ_p.

in the sense that the average over one period of $\psi_p(x) - Fx$ vanishes. In addition, it is crucial that ψ_p has exactly zero stretching energy, i.e. $\nabla\psi_p \in O(2,3)$ everywhere. Moreover, we have the bounds

$$|\psi_p(x) - Fx| \le cp{\epsilon_*}^{1/2}\,, \quad |\nabla\psi_p(x) - F| \le c{\epsilon_*}^{1/2}\,, \quad |\nabla^2\psi_p(x)| \le c\frac{{\epsilon_*}^{1/2}}{p}\,.$$

The energy per unit area is proportional to $h^2\epsilon_*/p^2$, and is entirely determined from the bending term in $I_{2\mathrm{D}}$. Such oscillatory maps do not, however, satisfy the affine Dirichlet boundary condition. Therefore one inserts a boundary layer, as illustrated in Figure 3. Precisely, we fix a small parameter ξ representing the width of the interpolation layer, and define

$$\psi(x) = \theta(x)\psi_p(x) + (1-\theta(x))Fx\,.$$

Here θ is a smooth interpolation function which equals zero outside ω, one on all points inside ω whose distance from the boundary is larger than ξ, and obeys the bounds $0 \le \theta \le 1$, $|\nabla\theta| \le c/\xi$, $|\nabla^2\theta| \le c/\xi^2$ everywhere, for some constant c which depends only on the domain ω. This generates a boundary layer whose area is controlled by ξ. There, the deformation gradient takes the form

$$\nabla\psi(x) = \nabla\theta(x)(\psi_p(x) - Fx) + \theta(x)\nabla\psi_p(x) + (1-\theta(x))F\,, \qquad (6)$$

and its stretching energy density is controlled by

$$\mathrm{dist}^2(\nabla\psi, O(2,3)) \simeq c{\epsilon_*}^2\left(1 + \frac{p^4}{\xi^4}\right)\,.$$

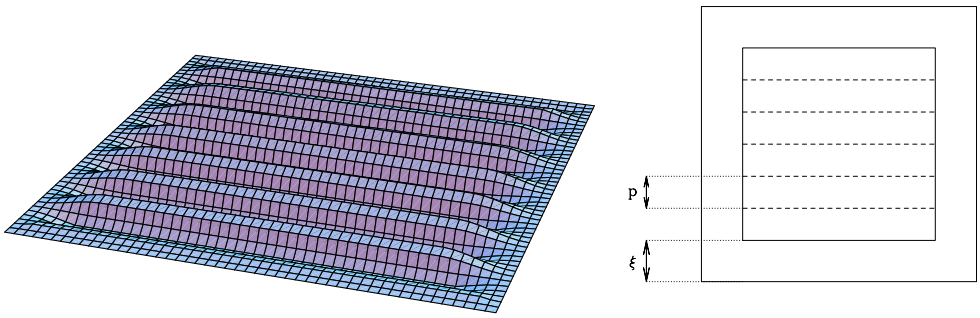

(a) (b)

FIGURE 3: Relaxing a uniaxial compression in a square. (a): resulting three-dimensional construction. (b): subdivision of the domain. The construction is p-periodic plus affine in the interior, and is given by the smooth interpolation in a ξ-neighborhood of the boundary.

To see this, observe that the second and third term in (6) correspond to an average between $\nabla\psi_p \in O(2,3)$ and F. Since $\mathrm{dist}(F, O(2,3)) = \epsilon_*$ and $|F - \nabla\psi_p| \leq c{\epsilon_*}^{1/2}$, it follows that the average is at a distance of order ϵ_* from $O(2,3)$. Further, the first two components of the first term in (6) are of order $p\epsilon_*/\xi$, and the third one of order $p{\epsilon_*}^{1/2}/\xi$. Therefore the first term modifies the distance from $O(2,3)$ only at order $\epsilon_*(p/\xi + p^2/\xi^2)$.

A similar analysis applies to the bending energy, which turns out to be of order $h^2|\nabla^2\psi|^2 \simeq c\epsilon_* h^2(1/\xi^2 + 1/p^2)$. The total energy of this construction can be therefore estimated as

$$E^{\mathrm{1D}} \leq c{\epsilon_*}^2\left(\xi + \frac{p^4}{\xi^3}\right) + c\epsilon_* h^2\left(\frac{1}{\xi} + \frac{\xi}{p^2}\right) + c\frac{\epsilon_* h^2}{p^2}\,,$$

where the last term is the bulk contribution $h^2|\nabla^2\psi_p|^2$. The optimal value of ξ is p, and gives for the total energy the estimate

$$E^{\mathrm{1D}} \leq c{\epsilon_*}^2 p + c\epsilon_* h^2\frac{1}{p} + c\frac{\epsilon_* h^2}{p^2}\,. \tag{7}$$

The optimal value of p is then determined by balancing the first and the last term, and results in $p = h^{2/3}/{\epsilon_*}^{1/3}$. The final energy estimate is

$$E^{\mathrm{1D}} \leq ch^{2/3}{\epsilon_*}^{4/3}\,.$$

Combining this construction with the previous one leads to a candidate solution for the problem of isotropic compression whose energy is proportional to $h^{2/3}$. To see this, consider for definiteness the unit square

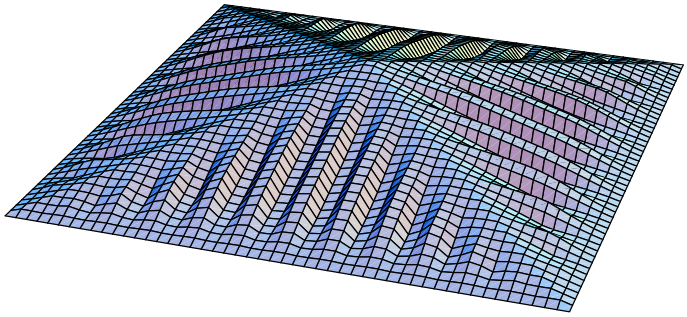

FIGURE 4: Deformation pattern obtained for isotropic compression in a square using one-dimensional oscillations in each of the four triangles. Note the separation of length scale between the roof-type construction which relaxes the isotropic compression to an uniaxial one, and the fine-scale oscillations which relax the remaining uniaxial compression.

$\omega = (0,1)^2$. The map obtained with the scalar approximation, i.e. (5) with $w(x) = (2\epsilon_* + {\epsilon_*}^2)^{1/2}\mathrm{dist}(x, \partial\omega)$, is affine on each of four pieces, as illustrated in Figure 1. In each of those triangles, the remaining uniaxial compression can be relaxed by fine-scale oscillations, which disappear by smooth interpolation approaching the boundary of the triangle. This ensures a smooth matching between the four pieces, and at the same time fulfillment of the boundary conditions. The resulting deformation is illustrated in Figure 4.

3.2 Optimal patterns beyond the one-dimensional construction: fold branching

The key competition determining the optimal total energy for the construction presented in the previous section is between the first term in (7), representing strain in the boundary layer and favoring fine-scale oscillations (i.e. small p), and the last one, representing bending energy in the bulk, and favoring coarse-scale oscillations (i.e. large p). This kind of competition is very common in problems in materials science where nonconvex bulk energies, with a regularizing singular perturbation (such as a wall energy or any higher-gradient term) compete with the boundary conditions. A pattern that makes an ubiquitous appearance in such problems is oscillation refinement towards the boundary, or, equivalently, coarsening towards the interior. Starting with the discussion of branched domains in the intermediate state of type-I superconductors by Landau back in 1938 [40, 41], and of magnetic

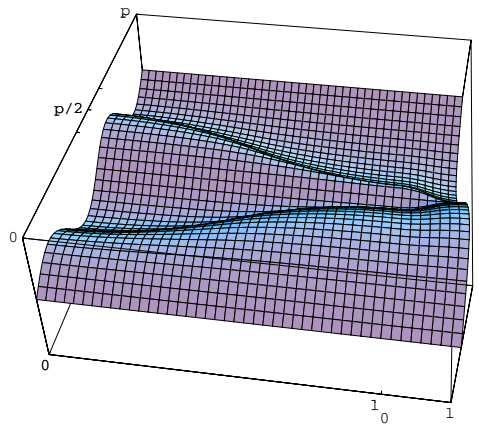

FIGURE 5: The period-doubling step of the construction. The period on the right is twice that on the left, the entire deformation is smooth and has small energy.

domains by Lifshitz in 1944 [45], self-similar constructions with a series of period-doubling steps have been used to construct low-energy states for a variety of models, and have in many cases found experimental confirmation. A heuristic one-dimensional model for the magnetic case was formulated by Hubert in 1967 [32], and the first mathematical results in this direction have been obtained for the case of shape-memory alloys by Kohn and Müller in 1992-1994 [37, 38], and later refined in [18, 19]. Their work originated a large amount of related mathematical investigations of pattern-formation problems in materials; similar domain branching has been demonstrated, beyond the blistering problem of interest here, in models of uniaxial ferromagnets [13, 15] of flux domain structures in the intermediate state of type-I superconductor plates [14], and dislocation walls in crystal plasticity [20, 19]. In the case of compressed thin films such branching patterns have been first used by Pomeau and Rica [54, 53], based on heuristic scaling estimates for the folding energies, followed by mathematical results in [8, 34, 35, 9]

The general idea is that fine-scale oscillations close to the boundary should be coupled to coarse-scale oscillations in the interior. The interpolation between the two can be achieved by means of a suitable period-doubling step, which for the blistering problem can be constructed as illustrated in Figure 5. Combining several such period-doublings at different scales one achieves deformations which interpolate between oscillations on very different length scales, as for example the one illustrated in Figure 6. In comparison to the estimate in (7), this construction permits to reduce substantially the last term (representing bending in the bulk) so that it disappears from the global en-

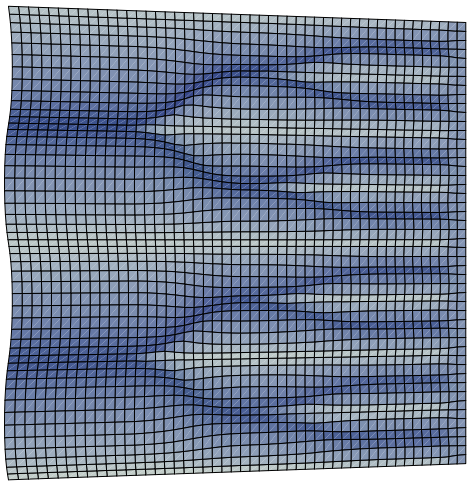

FIGURE 6: The explicit construction close to a straight boundary.

ergy balance. Then, the crucial competition is between the first two terms of (7), i.e. bending and stretching in the boundary layer, and gives $p = h/{\epsilon_*}^{1/2}$ and an energy scaling proportional to ${\epsilon_*}^{3/2}h$. This shows that the energy in the branching construction resides essentially in the boundary layers, which are localized both in a p-neighborhood of the exterior boundary $\partial\omega$ and in a p-neighborhood of the interior boundaries, given by the set of discontinuity points of $\nabla \mathrm{dist}(x, \partial\omega)$.

The construction sketched above can be made precise and extended to the full three-dimensional elasticity problem, for details see [9, 19]. We simply quote here the final result, which holds for smooth domains ω under the assumption that $W_{3\mathrm{D}}$ has globally at least quadratic growth, in the sense that

$$W_{3\mathrm{D}}(F) \geq c\,\mathrm{dist}^2(F, SO(3))\,, \tag{8}$$

and locally no more than quadratic growth, in the sense that there is $\delta > 0$ such that

$$W_{3\mathrm{D}}(F) \leq c'\mathrm{dist}^2(F, SO(3)) \qquad \text{for } \mathrm{dist}(F, SO(3)) \leq \delta\,. \tag{9}$$

We remark that since the upper bound (9) is only assumed to hold locally, the assumptions (8) and (9) are compatible with the behavior $W_{3\mathrm{D}}(F) \to \infty$ as $\det F \to 0$ and the constraint $\det F > 0$.

Theorem 1. *Let $\omega \subset \mathbb{R}^2$ be a bounded piecewise C^4 domain, and $W_{3\mathrm{D}}$ satisfy (8-9). Then, there are constants c_ω and C_ω depending only on ω such that for any $\epsilon_* \in (0, 1)$ and sufficiently small h one has*

$$c_\omega {\epsilon_*}^{3/2} h \leq \inf \frac{1}{h} \int_{\omega\times(0,h)} W_{3\mathrm{D}}(\nabla\phi) dx \leq C_\omega {\epsilon_*}^{3/2} h$$

where the infimum is taken over all maps $\phi : \omega \times (0,h) \to \mathbb{R}^3$ *which satisfy the boundary condition*

$$\phi(x) = \begin{pmatrix} (1-\epsilon_*)x_1 \\ (1-\epsilon_*)x_2 \\ x_3 \end{pmatrix}$$

for $(x_1, x_2) \in \partial\omega$*, and* $x_3 \in (0,h)$*.*

The proof of the upper bound is based on the extension of the construction discussed above to generic domain, and on a precise bookkeeping of all different energy contributions. Theorem 1 also contains a lower bound, which does not depend on any specific assumption on the deformation ('*ansatz-free lower bound*'). The proof of the lower bound builds upon the idea mentioned above, i.e., that the leading-order energy contribution is completely determined by the boundary layer alone, which corresponds to the first two terms in (7). To make this idea precise, one needs a rigidity result, that was derived by Friesecke, James and Müller in [29]. Precisely, one argues by contradiction, and shows that if there was a sequence of deformations with energy scaling less $h{\epsilon_*}^{3/2}$, then in the limit they would converge, in suitable subdomains close to the boundary, to an affine isometric deformation. But the latter cannot satisfy the boundary condition, giving the sought contradiction. Details of the proof are given in [9, 19].

We finally remark that the same scaling estimate holds with the three-dimensional elasticity replaced by the geometrically linear and geometrically nonlinear von Kármán energy, see [8, 9, 19]. A similar energy-scaling result has been independently obtained, for a related problem with partially Dirichlet and partially periodic boundary conditions, by Jin and Sternberg [34, 35] within the geometrically linear von Kármán model.

4 Anisotropic compression

In this section we extend the analysis to the case of anisotropic compression, restricting ourselves to the simplified scalar model. In 1994 Ortiz and Gioia [48] proposed to study the two-dimensional von Kármán energy by means of scalar deformations of the form (5), and obtained the simplified model I_{Eik}, as defined in (4), for the case of films under isotropic compression. The same approach can be extended in a natural way to the case of anisotropic compression, and indeed a first discussion in this direction appeared in [30], where experiments on compressed paper and plastic sheets have been presented, showing an interesting change in behavior between isotropically and uniaxially compressed sheets, see Figure 7.

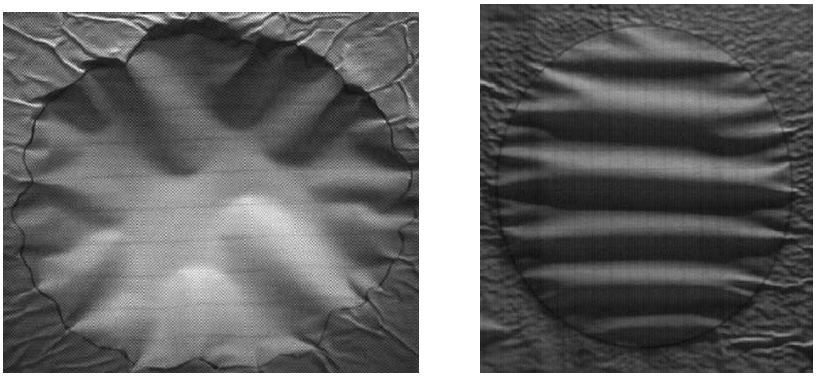

(a) (b)

FIGURE 7: Experimental pictures of compressed paper sheets, from [30]. (a): an isotropically compressed sheet, with $\epsilon_* = 0.04$ and $h/\operatorname{diam}\omega = 10^{-3}$. Folds start from the boundary and coarsen for various lengths towards the interior in a rather unstructured way. (b): a uniaxially compressed sheet, with $\epsilon_*^{(1)} = 0$, $\epsilon_*^{(2)} = 0.04$, and $h/\operatorname{diam}\omega = 0.5 \cdot 10^{-3}$. Folds are essentially normal to the direction of maximal compression, and coarsen in the interior.

We choose coordinates which diagonalize the average in-plane compression, and neglect possible superimposed rotations. Further, we focus from the beginning on the reduced two-dimensional problem. Precisely, we replace the boundary condition (2) with

$$\psi(x) = \begin{pmatrix} (1-\epsilon_*^{(1)})x_1 \\ (1-\epsilon_*^{(2)})x_2 \\ 0 \end{pmatrix} \text{ on } \partial\omega\,,$$

where the small parameters $\epsilon_*^{(2)} \geq \epsilon_*^{(1)} \geq 0$ represent compression in the x_2 and x_1 direction respectively. The one-dimensional *ansatz*, which now reads $\psi(x) = ((1-\epsilon_*^{(1)})x_1, (1-\epsilon_*^{(2)})x_2, w(x))$, leads to

$$I_{2\mathrm{D}}[\psi_{\mathrm{scal}}, \omega] \simeq \left(2\epsilon_*^{(1)}\right)^2 |\omega| + \left(2\epsilon_*^{(2)}\right)^2 I_{\sigma,\beta}\left[\sqrt{2\epsilon_*^{(2)}}w, \omega\right]$$

where the reduced functional

$$I_{\sigma,\beta}[u,\omega] = \int_\omega \left[(\nabla u)^2 - 1\right]^2 + 2\beta u_1^2 + \sigma^2 |\nabla^2 u|^2 \, dx$$

depends on the rescaled deformation $u = w\sqrt{2\epsilon_*^{(2)}}$ and on the parameters

$$\beta = \frac{\epsilon_*^{(2)} - \epsilon_*^{(1)}}{\epsilon_*^{(2)}}\,, \qquad \sigma = \frac{h}{(2\epsilon_*^{(2)})^{1/2}}\,.$$

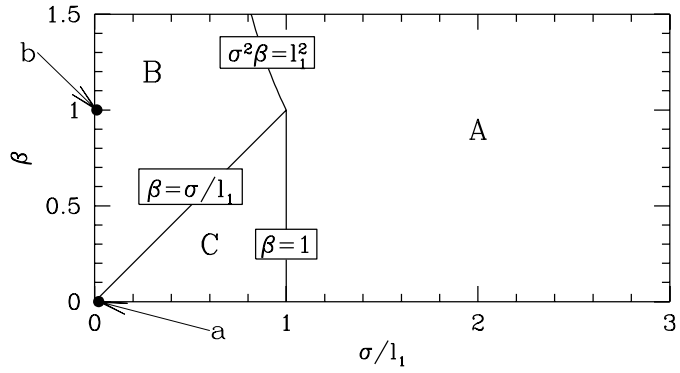

FIGURE 8: Phase diagram in the $(\sigma/l_1, \beta)$ plane as obtained from Theorem 2. Three regimes are present: in A the affine deformation is optimal, in B the branching pattern, in C the roof-type construction. See Figure 9 for the patterns and energy scalings. The two marked points $a = (0.004, 0)$ and $b = (0.002, 1)$ represent the position on this diagram of the experimental results of Figure 7.

(Here and below, $u_1 = \partial u/\partial x_1$.) For the case of isotropic compression, i.e. $\beta = 0$, this functional reduces to the Gioia-Ortiz eikonal functional I_{Eik} defined above.

The most interesting regime in the study of $I_{\sigma,\beta}$ is the one where both parameters are small, i.e., the limit in which the film is compressed in an almost isotropic way. We stress, however, that the results obtained with the scalar model should be seen only as a first approximation to the experimental situation, due to the mentioned differences in behavior between the scalar and the more realistic vectorial model.

For concreteness we shall consider a simple geometry, in which the domain is a rectangle, $R = (0, l_1) \times (0, l_2)$, with $l_2 \geq l_1$. As boundary condition, we shall impose $u = 0$ on the boundary ∂R. At this stage the problem has four independent real parameters: σ, β, l_1 and l_2. One of them (say, l_1) can be eliminated by rescaling. Indeed, if we let $u^\lambda(r) = \lambda u(r/\lambda)$ we get

$$I_{\sigma,\beta}[u, R] = \frac{1}{\lambda^2} I_{\lambda\sigma,\beta}[u^\lambda, \lambda R] \,.$$

Furthermore, for large l_2 we expect the limiting energy to be linear in l_2, hence we seek a phase diagram in the plane $(\beta, \sigma/l_1)$, and expect optimal energy scalings of the form $\inf I_{\sigma,\beta} \propto l_1 l_2 f(\sigma/l_1, \beta)$, which are valid for $l_2 \geq l_1$.

Figure 8 shows the resulting phase diagram, and Figure 9 illustrates the different patterns and energy scalings. If σ is large, precisely, if $\sigma > l_1$ and $\beta\sigma^2 > l_1^2$ (region A), the bending energy dominates and the trivial solution

$u = 0$ gives the optimal scaling of the energy, which is proportional to the area $l_1 l_2$. For $\sigma/l_1 < \beta < (\sigma/l_1)^{-2}$ (region B) a complex folding pattern develops. In the central part of the sample low-energy states have regions of alternating $u_2 \sim \pm 1$, whose width scales as $\sigma^{1/3} x_1^{2/3} \beta^{-1/3}$, separated by walls of width σ. Approaching the boundary the oscillation period decreases. This construction is essentially the same used in the previous section to relax the uniaxial compression. Finally, for $\beta < \sigma/l_1 < 1$ (region C) the functional behaves as I_{Eik}, and the optimal energy scaling is given by the smoothed distance to the boundary. The different patterns are illustrated in Figure 9. These results can be summarized in the following Theorem.

Theorem 2. *There are universal constants c and C such that in any rectangle $R = (0, l_1) \times (0, l_2)$ with $l_2 \geq l_1$ one has*

$$c f\left(\frac{\sigma}{l_1}, \beta\right) l_1 l_2 \leq \inf I_{\sigma,\beta}[u, R] \leq C f\left(\frac{\sigma}{l_1}, \beta\right) l_1 l_2$$

where the infimum is taken over functions $u \in W^{2,2}(R, \mathbb{R})$ which satisfy $u = 0$ on ∂R, and

$$f(x, y) = \min\left(1, \max(x, y), x^{2/3} y^{1/3}\right) .$$

As in Theorem 1, the upper bound can be obtained by making the sketched constructions precise, but the lower bound needs a different argument. In particular, the latter can be proven by contradiction using a compactness result obtained for the eikonal functional $I_{\mathrm{Eik}} = I_{\sigma,0}$ by Ambrosio, De Lellis and Mantegazza [2] and independently by DeSimone, Kohn, Müller and Otto [24]. This permits to show that a sequence whose energy would tend to zero faster than claimed in Theorem 2 would converge weakly to zero and, at the same time, strongly to a map whose gradient is everywhere of length one. But this is a contradiction. The complete argument is given in [19].

This result shows that the scalar approximation predicts two different regimes at small h. If the compression is isotropic, only the long-wavelength compression is captured by this approximation. The resulting pattern is smooth, and qualitatively well approximated by the distance function. The discussion in Section 3 shows that small-scale oscillations which refine towards the boundary are superimposed on a finer scale, and reduce the energy down to linear order in the thickness h. If instead the compression is approximately uniaxial, the scalar approximation predicts very different patterns, where no large-scale structure is present, but only fine-scale oscillations. The energy scaling is also in this case too high (the optimal energy scaling is linear in h, see [19]), but in both cases the scalar approximation correctly identifies the patterns associated with the largest length scale in the problem.

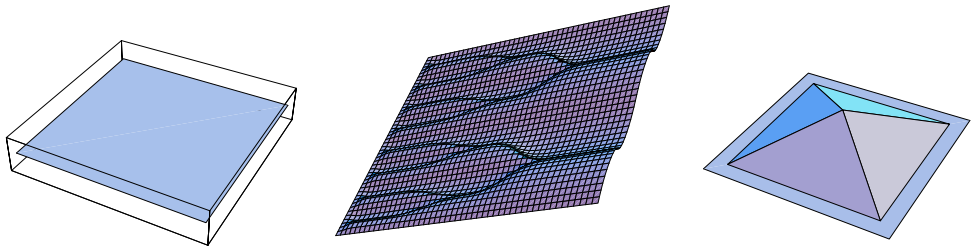

FIGURE 9: Illustration of the three different types of patterns found in the phase diagram of Figure 8, and corresponding energy scalings.

5 Concluding remarks

We have presented an analysis of the elastic problem arising in thin-film blistering from the viewpoint of the direct method of the (nonconvex) calculus of variations, which bypasses the Euler-Lagrange equations by focusing directly on qualitative properties of low-energy states. In particular, we have derived the optimal energy scaling by means of a combination of explicit constructions, for the upper bounds, and rigidity arguments, for the lower bounds. This approach is markedly different from the classical buckling-postbuckling analysis, which is based on the study of linear stability and of the leading nonlinear corrections. As already pointed out by Ortiz and Gioia [48], the regime in which many folds appear is well beyond the critical one for buckling. In particular, in a domain of size L the buckling threshold can be estimated by comparing the bending energy of the buckled state, proportional to $h^2\epsilon_*/L^2$ per unit area, with the energy of the (undistorted) affine deformation, which is proportional to ${\epsilon_*}^2$ per unit area. The buckling threshold, corresponding to loss of linear stability for the affine state, is $\sigma = L$. In typical experiments σ ranges from from a few percent of L to much less than L [48, 31], for example in the sheets represented Figure 7 we have $\sigma/L = 0.004$ and 0.002 respectively. Therefore blistering experiments explore the deeply nonlinear regime $\sigma \ll L$, named *folding regime* in [48], which is far from the buckling threshold and characterized by the formation of a large number of folds.

Acknowledgements

This work was partially supported by the Deutsche Forschungsgemeinschaft through the Schwerpunktprogramm 1095 *Analysis, Modeling and Simulation*

of Multiscale Problems.

References

[1] G. A. J. Amaratunga and M. E. Welland, *Electron beam defined delamination and ablation of carbon-diamond thin films on silicon*, J. Appl. Phys. **68** (1990), 5140–5145.

[2] L. Ambrosio, C. De Lellis, and C. Mantegazza, *Line energies for gradient vector fields in the plane*, Calc. Var. Partial Diff. Eqs. **9** (1999), 327–355.

[3] B. Audoly, *Stability of straight delamination blisters*, Phys. Rev. Lett. **83** (1999), 4124–4127.

[4] ———, *Mode-dependent toughness and the delamination of compressed thin films*, J. Mech. Phys. Solids **48** (2000), 2315–2332.

[5] P. Aviles and Y. Giga, *A mathematical problem related to the physical theory of liquid crystal configurations*, Proc. Centre Math. Anal. Austr. Nat. Univ. **12** (1987), 1–16.

[6] ———, *On lower semicontinuity of a defect energy obtained by a singular limit of the Ginzburg-Landau type energy for gradient fields*, Proc. Roy. Soc. Edin. A **129** (1999), 1–17.

[7] M. Ben Amar and Y. Pomeau, *Crumpled paper*, Proc. Roy. Soc. Lond. A **453** (1997), 729–755.

[8] H. Ben Belgacem, S. Conti, A. DeSimone, and S. Müller, *Rigorous bounds for the Föppl-von Kármán theory of isotropically compressed plates*, J. Nonlinear Sci. **10** (2000), 661–683.

[9] ———, *Energy scaling of compressed elastic films*, Arch. Rat. Mech. Anal. **164** (2002), 1–37.

[10] V. Berdichevskii and L. Truskinovskii, *Energy structure of localization*, Local effects in the analysis of structures (P. Ladevèze, ed.), Elsevier, 1985, pp. 127–158.

[11] A. Braides and A. Defranceschi, *Homogeneization of multiple integrals*, Claredon Press, Oxford, 1998.

[12] E. Cerda, S. Chaieb, F. Melo, and L. Mahadevan, *Conical dislocations in crumpling*, Nature **401** (1999), 46–49.

[13] R. Choksi and R. V. Kohn, *Bounds on the micromagnetic energy of a uniaxial ferromagnet*, Comm. Pure Appl. Math. **51** (1998), 259–289.

[14] R. Choksi, R. V. Kohn, and F. Otto, *Energy minimization and flux domain structure in the intermediate state of a type-I superconductor*, J. Nonlinear Sci, to appear.

[15] ———, *Domain branching in uniaxial ferromagnets: a scaling law for the minimum energy*, Comm. Math. Phys. **201** (1999), 61–79.

[16] P. G. Ciarlet, *A justification of the von Kármán equations*, Arch. Rat. Mech. Anal. **73** (1980), 349–389.

[17] ———, *Theory of plates*, Mathematical elasticity, vol. II, Elsevier, Amsterdam, 1997.

[18] S. Conti, *Branched microstructures: scaling and asymptotic self-similarity*, Comm. Pure Appl. Math. **53** (2000), 1448–1474.

[19] ———, *Low-energy deformations of thin elastic sheets: isometric embeddings and branching patterns*, Habilitation thesis, Universität Leipzig, 2003.

[20] S. Conti and M. Ortiz, *Dislocation microstructures and the effective behavior of single crystals*, in preparation.

[21] G. Dal Maso, *An introduction to* Γ*-convergence*, Birkhäuser, Boston, 1993.

[22] E. De Giorgi, *Sulla convergenza di alcune successioni d'integrali del tipo dell'area*, Rend. Mat. (IV) **8** (1975), 277–294.

[23] C. De Lellis and F. Otto, *Structure of entropy solutions: applications to variational problems*, J. Eur. Math. Soc. **5** (2003), 107–145.

[24] A. DeSimone, R. V. Kohn, S. Müller, and F. Otto, *A compactness result in the gradient theory of phase transitions*, Proc. Roy. Soc. Edin. A **131** (2001), 833–844.

[25] ———, *A reduced theory for thin-film micromagnetics*, Comm. Pure Appl. Math. **55** (2002), 1408–1460.

[26] N. M. Ercolani, R. Indik, A. C. Newell, and T. Passot, *The geometry of the phase diffusion equation*, J. Nonlinear Sci. **10** (2000), 223–274.

[27] G. Friesecke, R. James, and S. Müller, *A hierarchy of plate models derived from nonlinear elasticity by Gamma-convergence*, in preparation.

[28] ———, *Rigorous derivation of nonlinear plate theory and geometric rigidity*, C. R. Acad. Sci. Paris **334** (2002), 173–178.

[29] ———, *A theorem on geometric rigidity and the derivation of nonlinear plate theory from three dimensional elasticity*, Comm. Pure Appl. Math **55** (2002), 1461–1506.

[30] G. Gioia, A. DeSimone, M. Ortiz, and A. M. Cuitino, *Folding energetics in thin-film diaphragms*, Proc. Roy. Soc. London Ser. A **458** (2002), 1223–1229.

[31] G. Gioia and M. Ortiz, *Delamination of compressed thin films*, Adv. Appl. Mech. **33** (1997), 119–192.

[32] A. Hubert, *Zur Theorie der zweiphasigen Domänenstrukturen in Supraleitern und Ferromagneten*, Phys. Stat. Sol **24** (1967), 669–682.

[33] W. Jin and R. V. Kohn, *Singular perturbation and the energy of folds*, J. Nonlinear Sci. **10** (2000), 355–390.

[34] W. Jin and P. Sternberg, *Energy estimates of the von Kármán model of thin-film blistering*, J. Math. Phys. **42** (2001), 192–199.

[35] ———, *In-plane displacements in thin-film blistering*, Proc. R. Soc. Edin. A **132A** (2002), 911–930.

[36] G. Kirchhoff, *Über das Gleichgewicht und die Bewegung einer elastischen Scheibe*, J. Reine Angew. Math. **40** (1850), 51–88.

[37] R. V. Kohn and S. Müller, *Branching of twins near an austenite-twinned-martensite interface*, Phil. Mag. A **66** (1992), 697–715.

[38] ———, *Surface energy and microstructure in coherent phase transitions*, Comm. Pure Appl. Math. **47** (1994), 405–435.

[39] E. M. Kramer and T. A. Witten, *Stress condensation in crushed elastic manifolds*, Phys. Rev. Lett. **78** (1997), 1303–1306.

[40] L. D. Landau, *The intermediate state of supraconductors*, Nature **141** (1938), 688.

[41] ———, *On the theory of the intermediate state of superconductors*, J. Phys. USSR **7** (1943), 99.

[42] H. LeDret and A. Raoult, *Le modèle de membrane nonlinéaire comme limite variationelle de l'élasticité non linéaire tridimensionelle*, C. R. Acad. Sci. Paris **317** (1993), 221–226.

[43] ———, *The nonlinear membrane model as a variational limit of nonlinear three-dimensional elasticity*, J. Math. Pures Appl. **73** (1995), 549–578.

[44] ———, *The membrane shell model in nonlinear elasticity: a variational asymptotic derivation*, J. Nonlinear Science **6** (1996), 59–84.

[45] E. Lifshitz, *On the magnetic structure of iron*, J. of Phys. **8** (1944), 337–346.

[46] A. E. Lobkovsky, S. Gentges, Hao Li, D. Morse, and T. A. Witten, *Scaling properties of stretching ridges in a crumpled elastic sheet*, Science **270** (1995), 1482–1485.

[47] R. Monneau, *Justification of the nonlinear Kirchhoff-Love theory of plates as the application of a new singular inverse method*, Arch. Rat. Mech. Anal. **169** (2003), 1–34.

[48] M. Ortiz and G. Gioia, *The morphology and folding patterns of buckling-driven thin-film blisters*, J. Mech. Phys. Solids **42** (1994), 531–559.

[49] O. Pantz, *Une justification partielle du modèle de plaque en flexion par* Γ*-convergence*, C. R. Acad. Sci. Paris Série I **332** (2001), 587–592.

[50] ———, *On the justification of the nonlinear inextensional plate model*, Arch. Rat. Mech. Anal. **167** (2003), 179–209.

[51] A. C. Pipkin, *Continuously distributed wrinkles in fabrics*, Arch. Rat. Mech. Anal. **95** (1986), 93–115.

[52] ———, *The relaxed energy for isotropic elastic membranes*, IMA J. Appl. Math. **36** (1986), 85–99.

[53] Y. Pomeau, *Buckling of thin plates in the weakly and strongly nonlinear regimes*, Phil. Mag. B **78** (1998), 235–242.

[54] Y. Pomeau and S. Rica, *Plaques très comprimées*, C. R. Acad. Sci. Paris Ser. IIB **325** (1997), 181–187.